

# Measurement of 40 MeV Deuteron Induced Reaction on Fe and Ta for Neutron Emission Spectrum and Activation Cross Section

Toshiro Itoga, Masayuki Hagiwara, Takuji Oishi, So Kamada, Mamoru Baba

*Cyclotron and Radioisotope Center, Tohoku University, Aramaki, Aoba-ku, Sendai 980-8578, Japan*

With a view to improve the data accuracy, the neutron emission spectra and the activation cross section for the deuteron interaction with  $^{nat}\text{Ta}$ ,  $^{nat}\text{Fe}$  which will be used as the structural materials in IFMIF (International Fusion Materials Irradiation Facility), we have measured the 1) differential thick target neutron yields from thick tantalum and iron targets bombarded by 40 MeV deuterons, and the 2) excitation functions of activation cross sections for deuteron interaction with tantalum and iron up to 40 MeV, at the K=110 AVF cyclotron facility of Tohoku University.

## 1. Introduction

The International Fusion Material Irradiation Facility (IFMIF) project has been proposed to establish an accelerator-based d-Li neutron source in order to produce the intense fluence for test irradiations of fusion reactor candidate materials [1]. In IFMIF, high current (250 mA) deuteron beam is accelerated to 40 MeV and transported to the liquid lithium target so as to generate a neutron field that simulates a fusion reactor neutron field.

For the safety design and management of IFMIF, detailed knowledge is required on the neutron emission spectrum and the activation cross-section. The neutron flux and spectral data play an important role for accurate estimation of the neutron shielding, and the activation cross-section is indispensable for the estimation of radioactivity induced in the accelerator components and shielding materials. Although some studies had already been undertaken on these subjects, the data are scarce and the data accuracy is not good enough at present [2].

To improve the accuracy of the neutron energy-angular distribution data and the predictability of the radioactivity accumulation in IFMIF, we have been conducting a series of experiments on the neutron emission spectrum of the (d,xn) reaction and the activation cross-section and radioactivity induced in the accelerator components with the AVF cyclotron at the Tohoku University Cyclotron and Radioisotope Center (CYRIC). So far, we have obtained data on lithium targets for 25 and 40 MeV deuterons [3][4] and on carbon and aluminum targets for 40 MeV deuterons [5].

Here, we present the experiments on 1) neutron emission spectra from thick iron and tantalum, and 2) activation cross-sections of the  $^{nat}\text{Fe}(d,x)^{51}\text{Cr}$ ,  $^{nat}\text{Fe}(d,x)^{52}\text{Mn}$ ,  $^{nat}\text{Fe}(d,x)^{56}\text{Co}$ ,  $^{nat}\text{Fe}(d,x)^{57}\text{Co}$  and  $^{nat}\text{Fe}(d,x)^{58}\text{Co}$  reactions. These data are required for shielding design and radioactivity estimation since

these elements are one of the main accelerator components, especially in the beam tube. The neutron spectra were measured at seven laboratory angles between 0- and 110- deg. The stacked target technique was applied to obtain the activation cross-section from 40 MeV down to the threshold energy.

## 2. Experimental apparatus

The experiments were carried out using the AVF cyclotron at the Tohoku University CYRIC. The experimental apparatus is almost the same as one employed in Refs. 3-5. A deuteron beam accelerated to 40 MeV by means of cyclotron was transported to the NO.5 target room which was equipped with a beam-swinger system and a neutron flight channel that enabled angular distribution measurements without changing the detector arrangement [6]. The frequency of the deuteron beam was reduced to 2.3 MHz with a beam chopper to avoid a frame-overlap in the time-of-flight (TOF) measurements.

The thick iron and tantalum targets were set on a remotely-controllable target changer together with a beam viewer of a ZnS(Ag) scintillation sheet. The support frame was isolated from ground to read a beam charge induced on the thick target. To measure the number of incident particles accurately, a copper mesh biased to -500 V was installed around the target to suppress secondary electrons emission from the targets.

We adopted a two-detector method to obtain the data over almost the entire energy range of secondary neutrons [4-5,7]. Neutrons emitted from the targets were detected by an NE213 organic liquid scintillation detector, 14-cm-diam  $\times$  10-cm-thick or 2-inch-diam  $\times$  2-inch-thick, through a 1.5 m thick concrete-iron collimator which reduced the background events due to neutron scattering and  $\gamma$ -rays from activated components and the beam dump. The larger and smaller detectors were placed around 11.0 m and 3.5 m from the target, respectively. In the measurements with the longer flight path, an NE213 scintillation detector coupled with a Hamamatsu R1250 photo-multiplier and a tube base specially designed for high energy range neutrons [8] was employed to measure emitted neutrons over the whole energy region with high energy resolution. The shorter flight path was adopted to measure the low energy part of the neutron spectra with high gain avoiding the frame-overlap. The long and short path measurements covered 4.0 – 60 MeV and 0.5 – 5 MeV regions, respectively, of secondary neutron energy range. Using this technique, we obtained the data over almost the entire energy range of secondary neutrons with sufficient energy resolution and good signal-to-noise ratio.

The measurements of the neutron spectra were conducted at seven laboratory angles (0,5, 15, 30, 60, 90 and 110 deg.) with the beam swinger system. In each measurement, the TOF, pulse-shape-discrimination (PSD) and pulse-height data were collected event by event as three parameter list data for off-line analysis [3-5,7].

## 3. Target dimensions

The stacked targets were prepared to measure not only thick target neutron spectra but also the activation cross-section of (d,x) reactions for iron and tantalum. The stacked targets consist of twenty elemental iron (purity: 99.5 %) foils of approximately 30 mm  $\times$  30 mm  $\times$  100  $\mu$  m thick. The total

thickness (2 mm) is greater than the range calculated with the SRIM code [9] (1.72 mm in iron for 40 MeV deuteron) and thick enough to stop the incident beam.

#### 4. Experimental procedures

First, the neutron measurements were performed for 0-110 degree laboratory angles. During the irradiation, the beam current on the targets was continuously recorded using a multi-channel scalar (MCS) for normalization of the neutron TOF spectra and for the later activation measurements of the stacked targets. The beam current on the targets was around 2 nA and its pulse width was 2-3 ns is FWHM.

After the irradiation, the activities of  $^{51}\text{Cr}$ ,  $^{52}\text{Mn}$ ,  $^{56}\text{Co}$ ,  $^{57}\text{Co}$ ,  $^{58}\text{Co}$  accumulated in each stacked targets were measured by detecting 320.08 keV, 935.52 keV, 1238.26 keV, 122.06 keV and 810.76 keV,  $\gamma$ -rays, respectively, at 5 cm from the detector with a high-pure Ge detector (EURICIS MESURESE GPC50 -195-R) and a multi-channel analyzer. The dead times during the  $\gamma$ -ray counting were less than 2 %.

#### 5. Data analysis

##### 5.1 Neutron Spectra

Neutron TOF spectra were obtained by gating the neutron events with a pulse-height bias on two-dimensional pulse pulse-height vs. PSD graphical plots and by removing random background events to eliminate  $\gamma$ -ray events. The TOF spectra were converted into neutron energy spectra according to the Lorentz conversion [3-5,7].

The energy spectra were divided by the solid angle of the experimental arrangements, an integrated charge of the incident beam and the detection efficiency calculated by the Monte Carlo code SCINFUL-R [10]. Finally, the data were corrected for the attenuation in the air and the wall of a vacuum chamber by means of the total cross-section data of LA150 [11].

##### 5.2 Activation cross-section

The activation cross-section was determined from the peak counts of the  $\gamma$ -ray spectra and the number of projectile with data corrections for the decay, the peak efficiency of the Ge detector, the self-absorption effect in the samples and the beam current fluctuation during irradiation [3]. The efficiency curves were determined experimentally with standard  $\gamma$ -ray sources. The data were corrected for the energy degradation and the attenuation of incident particles through the targets. The incident energy for each stacked foil was estimated by the SRIM code [9].

#### 6. Results and Discussion

##### 6.1 Neutron spectra

For 40 MeV deuterons, the present results for the  $^{nat}\text{Fe}(d,xn)$  and  $^{nat}\text{Ta}(d,xn)$  neutron spectra at seven laboratory angles are shown in Fig.1. Figure 2, show the comparison of experimental data with the corresponding MCNPX calculation [12]. The data clarified secondary neutron production spectra for whole energy range. The lower energy limit is approximately 0.6 MeV. The error bars of the spectra

represent mainly the statistical errors. The 0-15 deg. spectra show main peaks centered around 15 MeV, similarly with the cases of previous experiments such as  $^{nat}\text{Li}(d,xn)$  reaction. Generally, these spectra have very strong angular dependence. It can be concluded that the neutrons are produced by similar reaction mechanisms on the main neutron peak region.

The  $^{nat}\text{Ta}(d,xn)$  spectra extended up to approximately 50 MeV though the  $^{nat}\text{Fe}(d,xn)$  spectra are limited to around 45 MeV. This is consistent with the reaction Q-value of 9.52 and 3.8 MeV for the  $^{nat}\text{Ta}(d,n)$  reaction and  $^{nat}\text{Fe}(d,n)$  reaction, respectively. Figure 2 shows the comparison with the results of MCNPX. The results of MCNPX underestimate the experimental data in whole energy region. In the case of 60 degree, the figure is almost same except for lower energy region. Figure 3 shows the comparison of neutron emission spectra from thick Li, C and Al with present data. In this figure, the neutrons from break-up reaction becomes lower while low energy neutrons increase with the increasing target mass. For the reason, lithium seems to be best for the neutron source due to its high neutron yield. Carbon is better material for beam dump due to low activities, although, neutron yield for carbon is larger than the other heavier nuclides.

## 6.2 Activation cross-section

The cross-section acquired for the  $^{nat}\text{Fe}(d,x)^{51}\text{Cr}$ ,  $^{nat}\text{Fe}(d,x)^{52}\text{Mn}$ ,  $^{nat}\text{Fe}(d,x)^{57}\text{Co}$  and  $^{nat}\text{Fe}(d,x)^{58}\text{Co}$  reactions are compared with other experimental data [13-18] with the evaluated data by the IAEA group [19] and calculations by a recent code TALYS [20]. Figure 4 shows the comparison for the  $^{27}\text{Fe}(d,x)^{51}\text{Cr}$  and  $^{52}\text{Mn}$  reaction. The present data is generally consistent with other experimental data. The TALYS results are similar to the experimental data in higher energy region, but they are much lower in magnitude. The present data for the  $^{nat}\text{Fe}(d,x)^{56}\text{Co}$ ,  $^{57}\text{Co}$  and  $^{58}\text{Co}$  reactions are consistent with other experimental data and the evaluated data except for the TALYS results as shown in Fig.5. To estimate radioactivity induced by deuterons with TALYS, improvements will be required for cross-section calculation models.

## 7. Summary

This paper described the experiments of (1) neutron energy-angular distribution from the Fe; Ta(d,xn) reactions and (2) cross-sections of the  $^{nat}\text{Fe}(d,x)^{51}\text{Cr}$ ,  $^{nat}\text{Fe}(d,x)^{52}\text{Mn}$ ,  $^{nat}\text{Fe}(d,x)^{56}\text{Co}$ ,  $^{nat}\text{Fe}(d,x)^{57}\text{Co}$  and  $^{nat}\text{Fe}(d,x)^{58}\text{Co}$  reaction performed using 40 MeV deuterons at Tohoku University CYRIC. In the neutron measurement, the spectra data for seven laboratory angles between 0-110 deg. were measured over almost the entire energy range from the maximum energy down to 0.7 MeV. These experimental results will be used as the basic data to check the accuracy of the Monte Carlo simulation and for the shielding design of tens of MeV accelerator facility such as IFMIF.

The activation cross-section data were acquired for iron from the threshold energy to 40 MeV. The data were generally consistent with other experimental data and evaluated data. However, the results by TALYS were generally much smaller than experimental values, while the shapes were similar to experimental values. The

presented results will be helpful for improvement of the calculation models.

## Reference

- [1]IFMIF CDA TEAM, IFMIF Conceptual Design Activity Final Report edited by Marcello Martone, Report 96.11, Enea, Dipartimento Energia, Frascati (1996)
- [2]M.A.Lone et al., Nucl. Instrum. and Meth., 143 (1977) 331
- [3]M. Baba, T. Aoki, M. Hagiwara et al., J. Nucl. Materials 307-311 (2002) 1715.
- [4]M., Hagiwara, et al., J. Nucl. Materials, 329-333, (2004) 218-222
- [5]T. Aoki, M. Hagiwara, M. Baba et al., J. Nucl. Sci. and Technol. 41 No.4 (2004) 399
- [6]Terakawa et al., Nucl. Instrum. Meth. A 491 (2002) 419.
- [7]T. Aoki, M. Baba, S. Yonai, N. Kawata, M. Hagiwara, T. Miura, T. Nakamura, Nucl. Sci. Eng., 146 (2004) 200
- [8]M. Baba, H. Wakabayashi, M. Ishikawa, T. Ito and N. Hirakawa, J. Nucl. Sci. and Technol., 27(No.7) (1990) 601
- [9]J. F. Ziegler, J. P. Biersack, U. Littmark, Pergamon Press, New York (1984).
- [10]S.Meigo Nucl. Instrum. Meth. A 401 (1997) 365
- [11]M. B. Chadwick, P. G. Young et al., Nucl. Sci. Eng. 131 (1999) 293
- [12]L.S. Waters (Ed.), MCNPX User's Manual version 2.4.0, LA-CP-02-408, Los Alamos National Laboratory, Los Alamos, New Mexico, 2002.
- [13]P. Jung, Conf. on Nucl. Data for Sci. and Technol., Juelich, 1991
- [14]J.W. Clark et al., Phys. Rev., 179, 1104
- [15]A. Hermanne et al., Nucl. Instrum. Meth. B, 161-163, 178
- [16]Zhao Wenrong et al., Chinese J. of Nuclear Physics Res., Sect. B, 17, 2, 163
- [17]J.W. Clark et al., Phys. Rev., 179, 1104
- [18]S.Takacs, et al., Conf.on Appl.of Accel.in Res.and Ind.,Denton,USA,1996
- [19]IAEA, Charged-particle cross section database for medical radioisotope production,  
<http://www-nds.iaea.org/medical/>
- [20]A.J. Koning, et al., TALYS: Comprehensive nuclear reaction modeling, Conf. on Nucl. Data for Sci. and Technol., Santa Fe, 2005

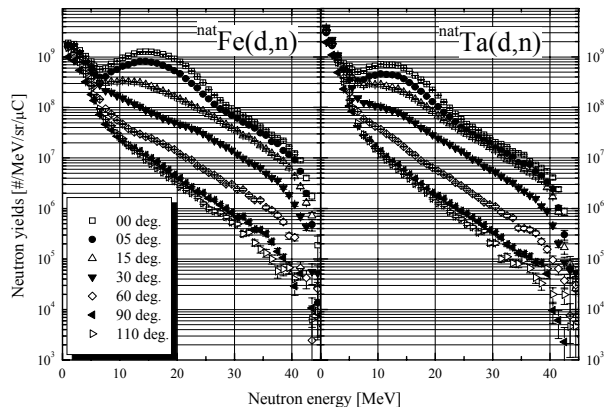


Fig. 1 Neutron spectrum for Fe and Ta

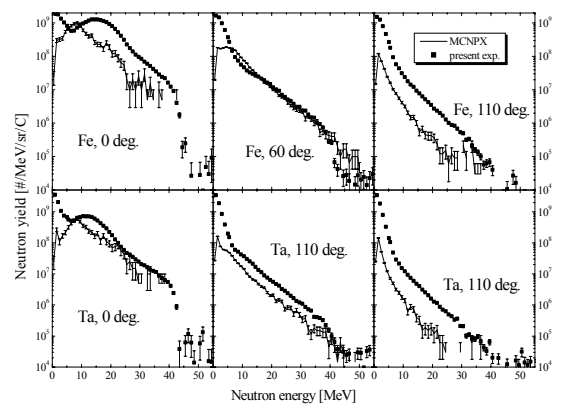


Fig. 2 Comparison with MCNPX

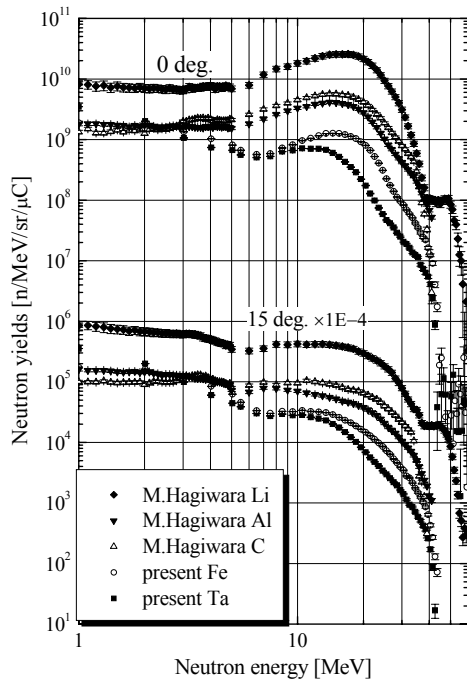


Fig. 3 Neutron spectrum for (d,n) reactions at 40 MeV

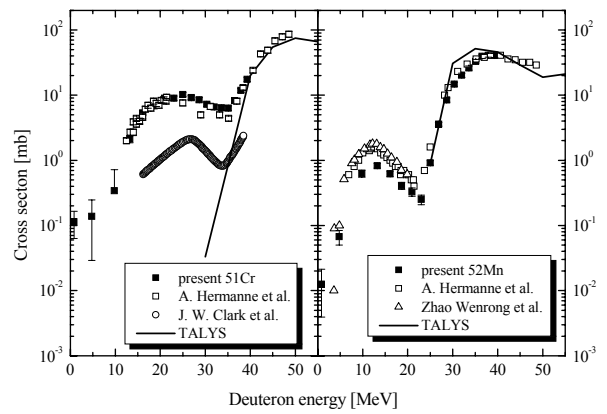


Fig. 4 Activation cross-section for  $^{nat}\text{Fe}(d, x)^{51}\text{Cr}, ^{52}\text{Mn}$

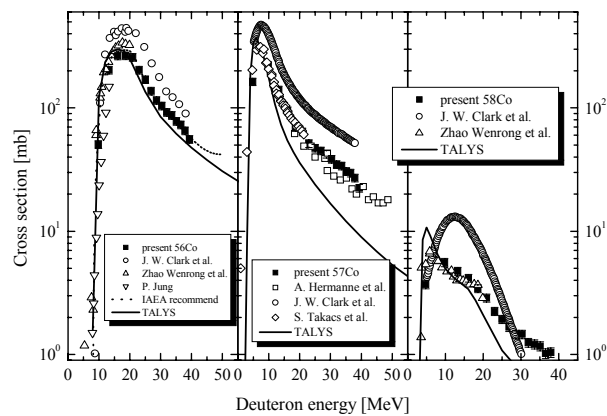


Fig. 5 Activation cross-section for  $^{nat}\text{Fe}(d, x)^{56}\text{Co}, ^{57}\text{Co}$  and  $^{58}\text{Co}$